

# CHEMISTRY

## A European Journal

A Journal of



### Accepted Article

**Title:** Metal-organic synthetic transporters (MOST): efficient chloride and antibiotic transmembrane transporters

**Authors:** Julie Kempf and Andreea R Schmitzer

This manuscript has been accepted after peer review and appears as an Accepted Article online prior to editing, proofing, and formal publication of the final Version of Record (VoR). This work is currently citable by using the Digital Object Identifier (DOI) given below. The VoR will be published online in Early View as soon as possible and may be different to this Accepted Article as a result of editing. Readers should obtain the VoR from the journal website shown below when it is published to ensure accuracy of information. The authors are responsible for the content of this Accepted Article.

**To be cited as:** *Chem. Eur. J.* 10.1002/chem.201700847

**Link to VoR:** <http://dx.doi.org/10.1002/chem.201700847>

Supported by  
**ACES**

WILEY-VCH

# Metal-organic synthetic transporters (MOST): efficient chloride and antibiotic transmembrane transporters

Julie Kempf,<sup>[a]</sup> and Andreea R. Schmitzer\*<sup>[a]</sup>

**Abstract:** We present the synthesis of two functionalized 2,4,7-triphenylbenzimidazole ligands and demonstrate the formation of their respective metal assemblies in phospholipid membranes. Anion transport experiments demonstrate the formation of metal-organic synthetic transporters (MOST) directly in phospholipid membranes. The formation of MOST in phospholipid membranes results in efficient architectures for chloride transport. We also demonstrate the insertion of these ligands and the formation of their metal-organic assemblies in bacterial membranes; the use of MOST makes the membranes of resistant bacteria more permeable to antibiotics. We also demonstrate that a combination of MOST with tetracycline lowers the sensitivity of resistant bacteria to tetracycline by 60-fold.

## Introduction

Metal-organic framework (MOF) materials are one of the most exciting, high-profile developments in nanotechnology in the last twenty years.<sup>[1],[2]</sup> Composed of metal nodes (metal ions, clusters, chains or layers) connected by organic linkers, they show some of the highest porosity known. This property is ideal for gas capture or storage<sup>[3]</sup> and drug delivery<sup>[4]</sup> applications. In particular, nontoxic and biodegradable MOFs have been used for the encapsulation and controlled delivery of a large number of therapeutic molecules, including several challenging antitumor and antiretroviral drugs such as busulfan, cidofovir and azidothymidine triphosphate.<sup>[5]</sup> In addition, metal-ligand assemblies (MLAs) are known to be capable of undergoing spontaneous reconstitution. This allows for the introduction of new functions in specific environments and is very attractive for mimicking the behavior of different biological systems involving metals.<sup>[6]</sup>

Ion transport across cell membranes is one of the most important processes in living cells and is regulated by a wide variety of transporters such as channels, mobile carriers and pumps.<sup>[7]</sup> There is a growing interest in understanding the mechanism of ion

transport and this has opened the door to the synthesis of a wide variety of synthetic ion transporters.<sup>[8]</sup> Nevertheless, the design of efficient synthetic ion transporters, and precise ion channels, remains a challenge. It is essential not only to predict the self-association of a compound into a pore-forming architecture, but also to understand the interactions with the surrounding membrane. For example, water or simple ions might interfere with and affect the integrity of the supramolecular architecture.<sup>[9]</sup> For this reason, the assembly of well-defined metal-organic channels in phospholipid bilayers may be a way to induce transmembrane transport.

Since functionalized platinum complexes have been shown to behave as metal-organic anion receptors in solution<sup>[10]</sup> and many anion receptors have been incorporated into the structure of transmembrane ion transporters, it is surprising that only a few MLAs or MOFs have been studied as ion transport candidates. Large MLAs such as Cu<sup>2+</sup>-based polyhedrons<sup>[11]</sup>, metal-oxide capsules<sup>[12]</sup> and oligo-porphyrins with Rh<sup>3+</sup>,<sup>[13]</sup> Pd<sup>2+</sup>,<sup>[14]</sup> or Zn<sup>2+</sup>,<sup>[15]</sup> were studied for their ionophoric properties. The large pores formed by the metal oligo-porphyrin assemblies were shown to be very effective for the transport of large molecules such as carboxyfluorescein or tetrabutylammonium cation across phospholipid bilayers. Due to the complexity of the synthetic pathway and the poor membrane insertion of these bulky assemblies, smaller components were designed to form synthetic ion channels by coordination with metals. The formation of the so-called "Fujita" motif between a bipyridine and an amphiphilic palladium derivative was studied by Fyles *et al.*<sup>[16]</sup> However, multiple unknown assemblies between this ligand and the metal were formed and the desired molecular square was not observed in the phospholipid membrane. Webb *et al.* also investigated pyridyl-palladium coordination for the formation of a reversible metal-organic channel in a phospholipid bilayer.<sup>[17]</sup> Addition of Pd<sup>2+</sup> to an amphiphilic cholate derivative resulted in a metal-ligand assembly that spanned the phospholipid bilayer and activated the proton/sodium transport process.

The assembly of discrete molecular units into extended networks is generally observed during MOF synthesis. Consequently, this synthetic approach allows reactions under mild conditions. Generally, little is known about the metal-ligand species preformed in solution before the assembly process. Therefore, MOFs are typically obtained by means of solvothermal synthesis.<sup>[18],[19]</sup> The similar *in situ* formation of a metal-organic synthetic transporter (MOST) in the phospholipid bilayer has yet to be demonstrated and exploited in transmembrane ion transport. This is presumably due to aqueous/membrane partitioning of the

[a] Dr. J. Kempf, Prof. Dr. A. Schmitzer  
Département de Chimie, Université de Montréal  
C. P. 6128 Succursale Centre-Ville, Montréal, Québec, H3C 3J7  
(Canada)  
Fax : (+1) 514-343-7586  
E-mail: [ar.schmitzer@umontreal.ca](mailto:ar.schmitzer@umontreal.ca)

Supporting information for this article is given via a link at the end of the document.

## FULL PAPER

ligand and the metal, as well as the presence of other ions can interfere with the assembly of the MOST.

We have previously demonstrated that 2,4,7-triphenylbenzimidazole **1** inserts into phospholipid bilayers and then self-assembles into rods that promote chloride transport (Figure 1).<sup>[20]</sup> With the addition of supplementary donor atoms (pyridine and carboxylate) on to this scaffold, we demonstrate herein how the assembly of MOSTs in the phospholipid bilayer, can be used to induce the transmembrane transport of ions and other molecules, particularly antibiotics. This is particularly important, as infections from resistant bacteria have become quite common, as more pathogens become resistant to multiple antimicrobials. Identification of new antibacterial agents and strategies as alternative treatments is crucial to increase our ability to fight infectious diseases.<sup>[21]</sup>

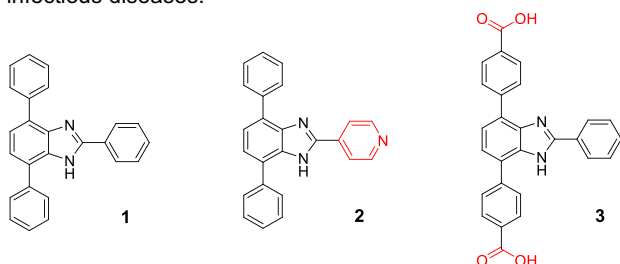


Figure 1. Structure of the 2,4,7-triphenylbenzimidazole (**1**) and its two analogues

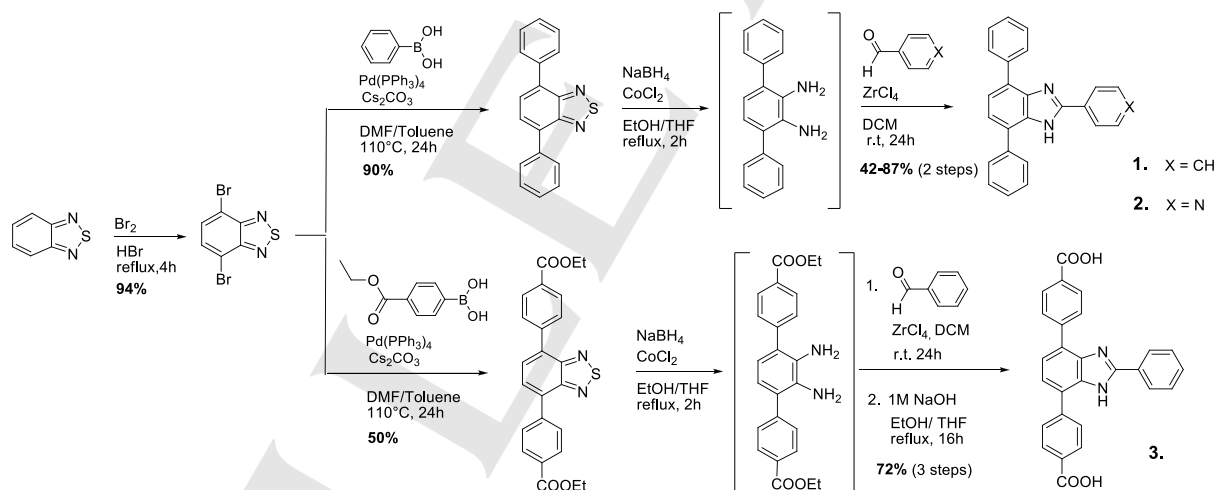
## Results and Discussion

## Synthesis

Ligands **2** and **3** were synthesized according to the previously reported procedure for **1**.<sup>[22]</sup> A pyridyl moiety was added in position 2 of the benzimidazole unit and two carboxylic acids were added in the *para* position of the aromatic rings to obtain ligands **2** and **3**, respectively. The synthetic pathway is shown in Scheme 1.

## Insertion into the phospholipid membrane

The insertion of ligands **2** and **3** into the phospholipid membrane, as well as the *in situ* formation of the MOST in a phospholipid membrane, were first monitored by fluorescence. Ligands were added to egg yolk phosphatidylcholine (EYPC) liposomes in a sodium/phosphate buffer (pH = 7.2).



Scheme 1. Synthesis of the ligands **1**, **2** and **3**.

As shown in Figure 2a, the maximum of fluorescence of **2** (in dichloromethane) was shifted from 440 nm to 435 nm when incorporated in the phospholipid bilayer, due to the stabilization of the excited state by the presence of a more polar environment (probably close to the charged groups of the phospholipids).<sup>[20]</sup> After addition of an aliquot of a PdCl<sub>2</sub> solution (in MeOH), a significant decrease of the fluorescence intensity was observed. This is likely the result of a re-organization of **2** in the membrane and formation of a metal-ligand complex, where photon transfer

from one molecule to another one spatially close can occur.<sup>[20]</sup> The same behavior was observed when PdCl<sub>2</sub> was added to ligand **3**, but the fluorescence quenching, induced by the addition of Pd<sup>2+</sup> ions, was less pronounced in this case suggesting a less dramatic structural change in the self-assembly of ligand **3** due to metal complexation (Figure 2b).

## FULL PAPER

## Formation of the metal-ligand complexes

Evidence for the formation of the metal-ligand complexes and their apparent stoichiometry were obtained by UV-vis titration. These experiments were performed in DCM in order to mimic the hydrophobicity of the phospholipid bilayer. Different amounts of  $\text{PdCl}_2$  were added to the ligand solution to monitor the complexation. In the case of ligand **1**, a 1:1 complex was formed by complexation of  $\text{Pd}^{2+}$  by the benzimidazole moiety, as indicated by the shift of the absorption band corresponding to the  $n\text{-}\pi^*$  transition, to shorter wavelengths<sup>[23]</sup> (see ESI, Figure S1). When  $\text{PdCl}_2$  was added to ligand **2** (Figure 3a), coordination of the more accessible pyridyl unit occurs, translated into a red shift of the band corresponding to the  $n\text{-}\pi^*$  transition at 318 nm. This is characteristic of the formation of pyridine:palladium complexes,<sup>[24]</sup> where the formation of a 2:1 complex is favored (Figure 3a). A 1:1 complex is formed upon addition of 1 equivalent of  $\text{PdCl}_2$  to ligand **3** (Figure 3b). The proposed structures of the palladium complexes formed in an apolar environment are shown in Figure 4. UV-vis titrations were also performed with  $\text{HAuCl}_4$ ,  $\text{AgBF}_4$ ,  $\text{RuCl}_3$  and  $\text{Pd}(\text{OAc})_2$  and the stoichiometry of the complexes are summarized in Table 1 (UV-vis spectra are provided in Figures S2-S9). Ligand **2** forms 2:1 complexes with  $\text{Pd}^{2+}$  and  $\text{Au}^{3+}$  and 1:1 complexes with  $\text{Ru}^{3+}$  and  $\text{Ag}^+$ . Ligand **3** forms complexes with a 1:1 general stoichiometry, which may also correspond to higher 2:2, 3:3 or  $n:n$  stoichiometries, with all the studied metals. However, addition of other metals than palladium to ligand **3**, resulted in the formation of different complexes with the benzimidazole unit, as a shift corresponding to the  $n\text{-}\pi^*$  transition band was observed (ESI Figures S3, S5, S7 and S9).

Formation of metal-ligand assemblies in the presence of liposomes was also monitored by UV-vis. The UV-vis spectra of both ligands **2** and **3** in the presence of liposomes are indistinguishable from those obtained in DCM, confirming their insertion in the apolar environment of the phospholipid membrane. When 0.5 equivalents of  $\text{PdCl}_2$  were added to the liposomes solution containing ligands **2** or **3**, a red shift of the band corresponding to the  $n\text{-}\pi^*$  transition was observed. In the case of ligand **2**, the increase in the amount of palladium to one equivalent did not induce any further change, compared to ligand **3**, where an increase of absorption at 323 nm was observed after addition of 0.67 equivalents of  $\text{PdCl}_2$  (Figure 5). Unfortunately, at higher concentrations of  $\text{PdCl}_2$  precipitation occurred in these aqueous conditions, the 1:1 conditions not having been reached.

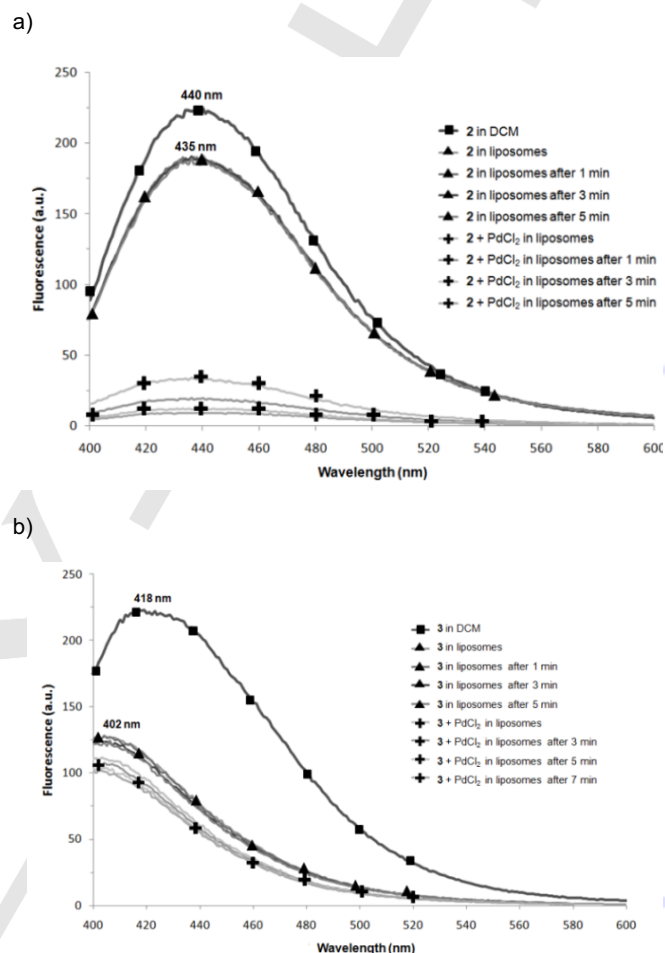


**Figure 2.** Fluorescence of a) **2** and b) **3** in dichloromethane (DCM) (0.016 mM, squares), in liposomes at 25 °C (15 mol%, triangle) and after the addition of 0.5 equivalents of  $\text{PdCl}_2$  (relative to the concentration of **2** and **3** respectively, crosses). Intravesicular solution: 500 mM  $\text{NaCl}$ , 5 mM phosphate buffer. Extravesicular solution: 500 mM  $\text{NaNO}_3$ , 5 mM phosphate buffer (pH = 7.2)

## FULL PAPER

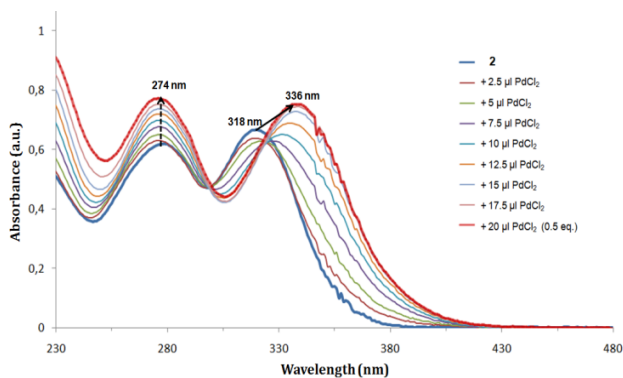
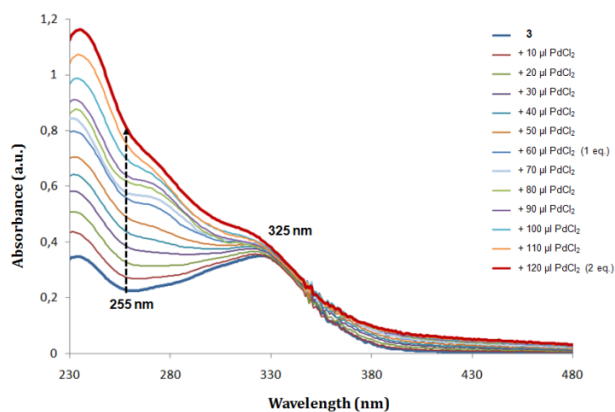


**Figure 3.** UV-Visible spectra of: a) **2** and b) **3** (concentration 0.033 mM) in  $\text{CH}_2\text{Cl}_2$  in presence of various concentrations of  $\text{PdCl}_2$  (methanol solution at 2.5 mM). The number of equivalents of  $\text{PdCl}_2$  reported in the legend are relative to the ligands.

**Table 1.** Stoichiometry of the complexes formed by **1**, **2** and **3** with different metals

	$\text{PdCl}_2$	$\text{Pd}(\text{OAc})_2$	$\text{RuCl}_3$	$\text{HAuCl}_4$	$\text{AgBF}_4$
<b>1</b>	1:1	n.d	n.d	n.d	n.d
<b>2</b>	2:1	2:1	1:1	2:1	1:1
<b>3</b>	1:1	1:1	1:1*	1:1*	1:1*

\*Metal complex formed with the benzimidazole moiety

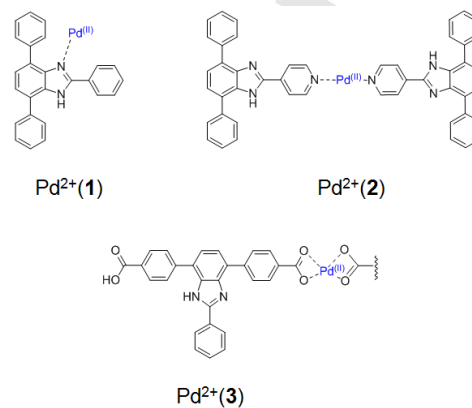


**Figure 4.** Schematic representation of the metal complexes of **1**, **2** and **3** with palladium. Chloride ions and coordinated solvents are not shown.

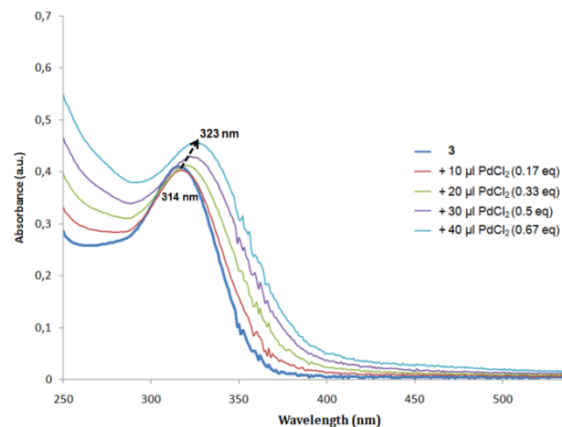
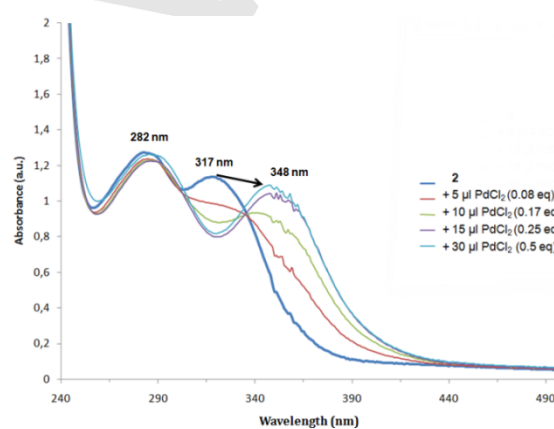


**Figure 5.** UV-visible spectra of **2** and **3** (final concentration 0.05 mM) in an aqueous solution of liposomes (5 mM) in the presence of different amounts of  $\text{PdCl}_2$

The palladium complex obtained upon the addition of 0.5 equivalent of  $\text{PdCl}_2$  to ligand **2** in acetonitrile was isolated as a dark orange powder and characterized by NMR (Figure S11). Upon complexation with  $\text{PdCl}_2$  a significant change in the  $^1\text{H}$  NMR

## FULL PAPER

spectra was observed, since the signal of the *ortho* and *meta* protons of the pyridine nitrogen were significantly shifted downfield. Due to the lack of solubility of ligand **3** in acetonitrile and of  $\text{PdCl}_2$  in DMSO, the formation of the complex of **3** with  $\text{Pd}(\text{OAc})_2$  was monitored in DMSO. Addition of 0.1 equivalents of Pd resulted in the appearance in the  $^1\text{H}$  NMR spectra of a sharp peak corresponding to the carboxylic proton. However, upon addition of 0.2 equivalents of  $\text{Pd}(\text{OAc})_2$  a precipitate was formed and surprisingly instant gel formation was observed when a 0.5 equimolar amount of  $\text{Pd}(\text{OAc})_2$  was added. Gel formation was confirmed by the vial inversion technique. The fast gelation process suggests that there is a rapid complexation between the palladium and the carboxylates, giving rise to large aggregates. Interestingly, ligand **2** gave the same supramolecular gelation under the same conditions, upon addition of 0.5 equivalents of  $\text{Pd}(\text{OAc})_2$  in DMSO. The morphological properties of these metallogels were studied through scanning electron microscopy (SEM) (Figure 6). Both palladium complexes form large fibers that exhibit fine structure and appear to be multi-layered. The fibers are relatively straight with only slight twisting, which is more pronounced in the case of **3**. Regular shape indicates that the fibers are formed by well-ordered molecular packing. The smallest fibers have an approximate width of 40 nm. The small fibers are layered together into thicker bundles of long fibers that have an approximate width of 0.3  $\mu\text{m}$ . The regular shape and the extreme ratio between width and length in this system must arise from a strong anisotropic growth process resulting in the possible presence of 1-D or 2-D structures in the system.

We previously reported the crystal structure of ligand **1**.<sup>[20]</sup> Unfortunately, crystals suitable for X-ray analysis were obtained only for ligand **2** by dissolving it in hot acetonitrile and subsequent slow evaporation of the solvent (see ESI). The supramolecular organization of **2** in the solid state reveals the formation of an aromatic channel, where the repeating unit is a dimer (Figure 7a). Starting with this structure, models were generated for the  $\text{Pd}^{2+}(\mathbf{2})$ , **3** and  $\text{Pd}^{2+}(\mathbf{3})$  using the PM6/SCF-MO method (Figure 7a). In a second step, the energy minimized  $\text{Pd}^{2+}(\mathbf{2})$  and  $\text{Pd}^{2+}(\mathbf{3})$  complexes were placed in a phosphatidylcholine bilayer and a 200 ps molecular dynamics study was performed. As shown in Figure 7b, both resulting palladium complexes possess porous structures, compared to the self-assemblies of the ligands alone.

The  $\pi$ - $\pi$  interactions observed for **2** in the crystal are no more the governing interactions, but *CH*- $\pi$  interactions become the major interactions in the metal complexes. In the case of ligand **3**, oligomers are formed through the coordination of palladium to the carboxylic acids, compared to the complexed palladium on the pyridine groups in the case of **2**.  $\text{Pd}^{2+}(\mathbf{2})$  complex remains embedded in the hydrophobic part of the bilayer, while  $\text{Pd}^{2+}(\mathbf{3})$  complex spans the entire bilayer, with the carboxylic acids exposed to the hydrophilic portion of the phosphatidylcholine layer.

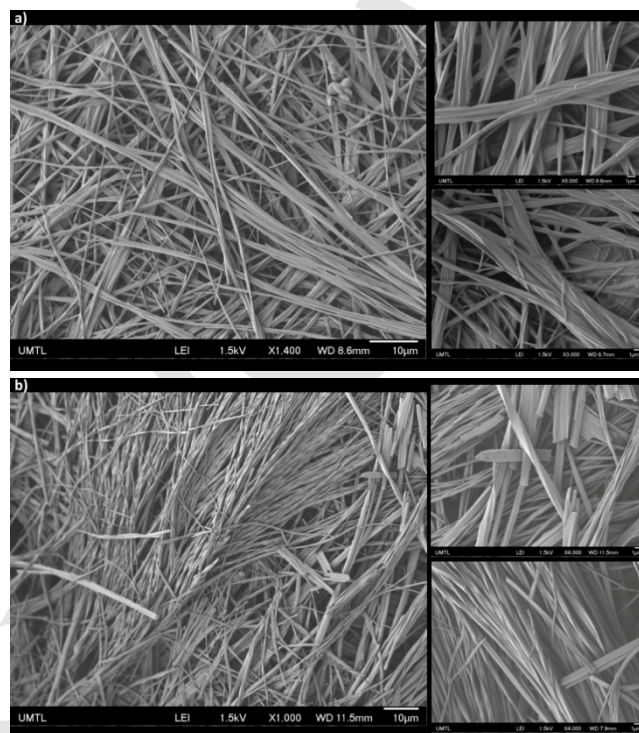


**Figure 6.** SEM images of hierarchically self-assembled gel microstructures (dried samples): a)  $\text{Pd}^{2+}(\mathbf{2})$  and b)  $\text{Pd}^{2+}(\mathbf{3})$ .

Both palladium complexes form rectangular prism structures in the phospholipid bilayer by the self-assembly of several palladium dimers (in the case of **2**) or oligomers (in the case of **3**). Three monomers are required in the case of  $\text{Pd}^{2+}(\mathbf{3})$  to span the entire bilayer, while in the case of  $\text{Pd}^{2+}(\mathbf{2})$  four monomers self-assemble to form the length of the rectangular prism. These models can be used to interpret the observed self-association of  $\text{Pd}^{2+}(\mathbf{2})$  and  $\text{Pd}^{2+}(\mathbf{3})$  into long fibers and bundles. Importantly, the formation of these types of self-assembled structures can be seen as the type of organized repeating unit that have the potential to produce a gel (Figure 7c) and help to rationalize the self-association of metal-ligand assemblies in the polarized environment of the phospholipid bilayer.

## FULL PAPER

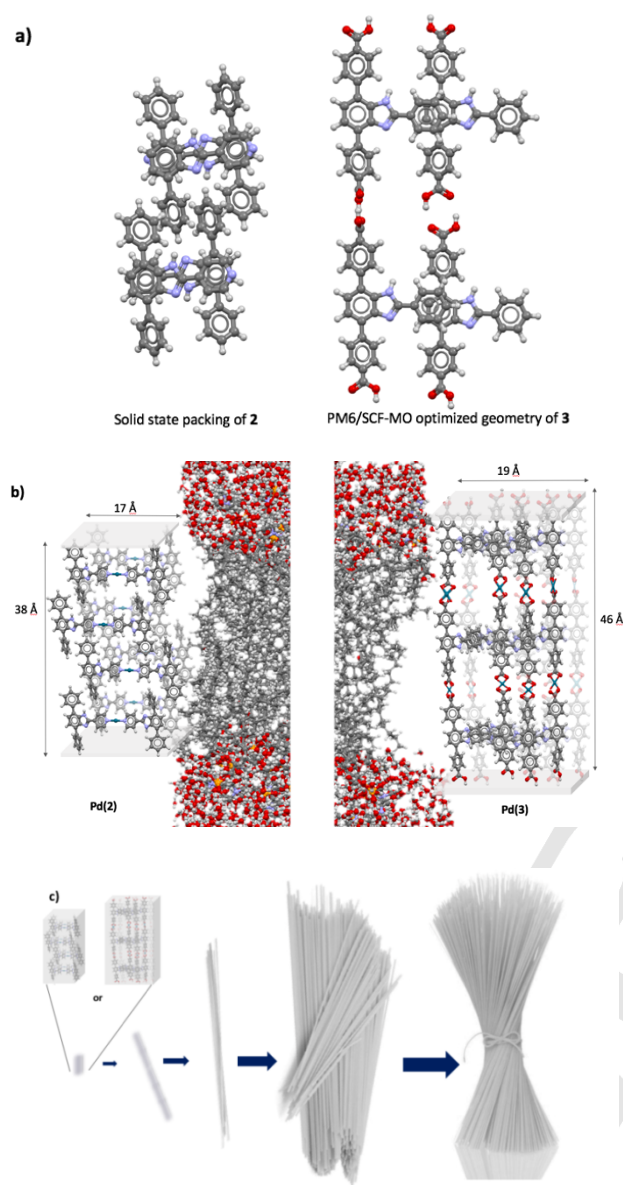


**Figure 7.** Molecular modeling: a) Crystal packing of **2** and PM6/SCF-MO optimized geometries of **3** in the gas phase. b) Palladium complexes Pd<sup>2+</sup>(**2**) and Pd<sup>2+</sup>(**3**) in an EYPC bilayer after a 200 ps molecular dynamics simulation. The resulting metal-ligand complexes were extracted from the phospholipid bilayer for clarity and only a partial view of the phospholipid is shown. c) Proposed hierarchical association in the gel.

### Chloride transport

Having previously reported the anionophoric properties of **1**,<sup>[20]</sup> we investigated the ability of **2**, **3** and their respective metal complexes to induce anion transport across a synthetic phospholipid membrane. Chloride transport studies were performed in the same EYPC large unilamellar liposomes (LUVs). The intravesicular solution of the liposomes was 5 mM phosphate buffer with 500 mM NaCl (pH = 7.2) and the chloride efflux mediated outside the liposomes was measured with a chloride-selective microelectrode. Kinetic experiments were carried out by varying the concentration of ligands from 2.5 mol% to 25 mol% relative to the EYPC concentration (5 mM). The quantity of chloride released in the extravesicular solution (5 mM phosphate buffer and 500 mM NaNO<sub>3</sub>, pH = 7.2) was directly correlated to the efficiency of the compound to mediate chloride transport. At the end of the experiment, a solution of Triton X was used to lyse the liposomes and record the maximum of chloride efflux. Based on these kinetic results, a Hill plot analysis was performed to determine the half-maximum effective concentration of the compounds after 500 seconds (EC<sub>50,500s</sub>) at 25 °C.

The structural modifications of the 2,4,7-triphenylbenzimidazole scaffold affected the transport efficiency, as the EC<sub>50,500s</sub> values were respectively 0.34 mM (6.9 mol% relative to EYPC concentration) for **1**, 1 mM (20.0 mol%) for **2** and 0.63 mM (12.6 mol%) for **3** (See ESI, Figures S14 – S19). In the case of ligand **1**, addition of palladium did not induce any major change in the transport properties (see ESI Figure S20), however, a completely different scenario occurred when metals were added to ligands **2** and **3**. For example, the addition of 0.5 equivalent of PdCl<sub>2</sub> (relative to the concentration of **2**) at 270 s after the chloride efflux was initiated by **2**, resulted in the assembly of an active MOSTs in the phospholipid bilayer and an increase in transport efficiency. Initially, metals (0.5 equivalent relative to **2**) that were previously used to perform UV-vis titrations were studied for their efficiency to form MOSTs in the phospholipid bilayer. An increase of chloride efflux was observed in presence of the Pd<sup>2+</sup> and Ru<sup>3+</sup>, compared to **2** alone. Although HAuCl<sub>4</sub> and AgBF<sub>4</sub> were able to form a complex with **2** in apolar solvents, their solubility in the extravesicular aqueous solution limited their insertion in the hydrophobic part of the phospholipid membrane and prevented the formation of the MOSTs. Consequently, only PdCl<sub>2</sub> and RuCl<sub>3</sub> were studied for further transport experiments.

## FULL PAPER

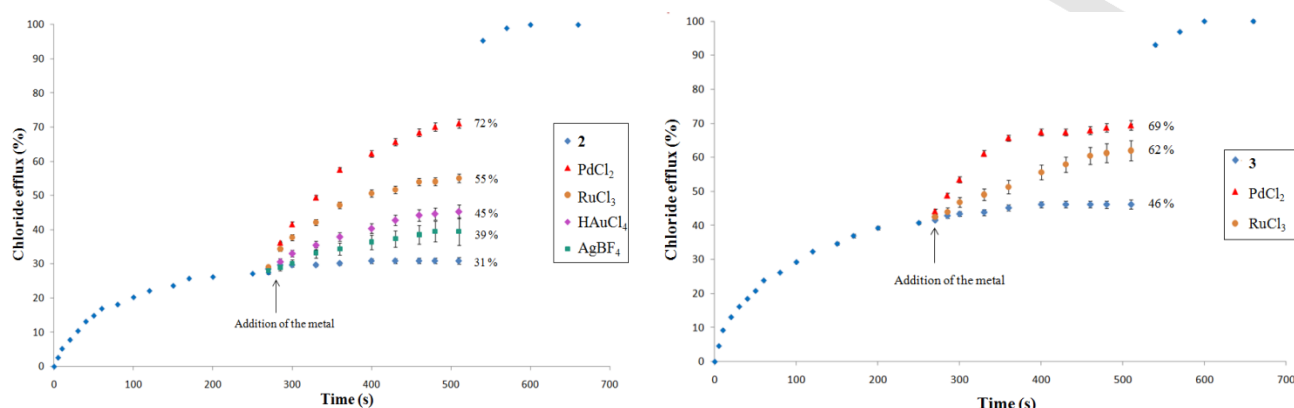


**Figure 8.** Chloride efflux obtained after the addition of 0.5 equivalents of different metal sources (relative to the concentration of ligand) at 270 s in the presence of 12.5 mol% (relative to the EYPC concentration) of **2** (left) and **3** (right) in liposomes at 25 °C. Triton X was added at 525 s to lyse the liposomes.

The addition of the Pd<sup>2+</sup> and Ru<sup>3+</sup> to **3** resulted in the same increase of the chloride efflux rate, demonstrating the assembly of the MOSTs in the phospholipid bilayer (Figure 8). For both ligands, the most efficient MOSTs were assembled with palladium. Different amounts of PdCl<sub>2</sub> were added at 270 s during the chloride transport experiment in presence of the three ligands and the maximums of chloride efflux at 500 s are reported in Table 2. Addition of the metals alone only induced a slight chloride efflux (Figures S26 and S31). It is important to underline that the increase in chloride efflux is not due to the presence of a higher concentration of chloride (displaced from the palladium complex by the solvent), as only 0.015 mM chloride could be generated from the 2.5 mM PdCl<sub>2</sub> (the highest concentration used), compared to the 500 mM NaCl present in the extravascular solution.

No significant influence of the amount of Pd<sup>2+</sup> was observed in the case of **1**. A maximum of chloride efflux was obtained when 0.5 equivalents of PdCl<sub>2</sub> were added to ligand **2**, showing the formation of a 2:1 stoichiometry in the MOST. Addition of 1 equivalent of PdCl<sub>2</sub> to **3** (required to form the 1:1 complex previously observed by UV-vis) did not increase the chloride efflux, suggesting the formation of a 2:1 complex inside the phospholipid membrane. Consequently, the same experiment was repeated with RuCl<sub>3</sub> confirming the formation of the 2:1 metal-ligand assembly in the phospholipid membrane with **2** and **3** (see ESI, Figures S32 and S33). Thus, in the phospholipid membrane, only 0.5 equivalent of metal (Pd<sup>2+</sup> or Ru<sup>3+</sup>) is necessary to assemble active MOSTs. This result, put together with the molecular modeling results (where a 3:2 complex was formed in the phospholipid bilayer) and the adduct observed by mass spectrometry (Figure S13), suggests the formation of stable 2:1 complexes in solution and oligomers of higher stoichiometry in the phospholipid bilayer.

**Table 2.** Chloride efflux at 500 s obtained after the addition of different concentrations of PdCl<sub>2</sub> at 270 s in presence of **1**, **2** and **3**

Ligand	No. of equiv. of PdCl <sub>2</sub> (added at 270 s)	% Cl efflux (measured at 500 s)
<b>1</b>	0	41 ± 3
	0.5	50 ± 3
	1	50 ± 5
<b>2</b>	0	31 ± 2
	0.25	53 ± 2
	0.5	74 ± 4
<b>3</b>	1	75 ± 5
	0	41 ± 2
	0.25	56 ± 4
<b>3</b>	0.5	69 ± 3
	1	69 ± 5

Additional kinetic experiments were carried out to extract the EC<sub>50,500s</sub> for each MOST. Transmembrane chloride transport was initiated by addition of **1**, **2** and **3** and 0.5 equivalent of PdCl<sub>2</sub> at 270 s. The maximum of chloride efflux obtained at 500 s was measured and a new Hill analysis was performed. The EC<sub>50,500s</sub> obtained for Pd(**1**), Pd<sup>2+</sup>(**2**) and Pd<sup>2+</sup>(**3**) were respectively 0.35 mM (7.0 mol%), 0.47 mM (9.5 mol%) and 0.54 mM (10.9 mol%). The chloride efflux induced by Pd<sup>2+</sup>(**2**) was increased from 31 to 75 %,

## FULL PAPER

while that induced by Pd<sup>2+</sup>(**3**) was increased from 41 to 69 % (see ESI, Figures S20 – S25).

We also performed chloride transport experiments with the preformed metal-organic complex for ligands **2** and **3**. Complexes Pd<sup>2+</sup>(**2**) and Pd<sup>2+</sup>(**3**) were initially prepared in methanol and added to the liposome solution. As shown in Table 3, the preformed complexes did not induce the same chloride efflux as the MOST assembled *in situ* in the phospholipid bilayer. This suggests that the preformed complexes are not stable in the extravesicular aqueous solution, as the chloride efflux is very similar to that obtained with the ligand alone. To confirm this hypothesis, a new aliquot of 0.5 equivalent of PdCl<sub>2</sub> was added 270 s after the addition of the preformed Pd<sup>2+</sup>(**2**). An increased chloride efflux was observed, reaching the same maximum as the previous ones, confirming that the initially preformed complex disassembles in aqueous media; the ligand alone permeates the bilayer and when additional PdCl<sub>2</sub> is added, the MOST is formed directly in the phospholipid bilayer.

We also confirmed by UV-vis spectroscopy that only 15 % of the preformed Pd<sup>2+</sup>(**2**) penetrates the phospholipid bilayer. The entire formation of the complex can only be achieved through addition of an additional aliquot of PdCl<sub>2</sub> (see ESI Figure S10). An intermediate transport efficiency was obtained with the preformed Pd<sup>2+</sup>(**3**), which confirms its higher stability in aqueous media.

**Table 3.** Chloride efflux at 500s obtained for ligands **2**, **3** and their respective preformed complex Pd<sup>2+</sup>(**2**) and Pd<sup>2+</sup>(**3**), with or without the addition of PdCl<sub>2</sub> at 270 s.

	% Cl <sup>-</sup> Efflux (at 500 s)	
	Without PdCl <sub>2</sub>	Upon addition of 0.5 eq. of PdCl <sub>2</sub> at 270 s
<b>2</b>	30 ± 1	74 ± 4
Preformed Pd <sup>2+</sup> ( <b>2</b> )	30 ± 2	68 ± 5
<b>3</b>	41 ± 1	67 ± 3
Preformed Pd <sup>2+</sup> ( <b>3</b> )	53 ± 3	68 ± 2

In order to determine the mechanism of the chloride efflux induced by the MOSTs, transport experiments were performed in 7/3 EYPC/cholesterol liposomes. Cholesterol rigidifies and orders the membrane by increasing the energy barrier of the movement of phospholipid inside the bilayer (rotation, lateral diffusion or phospholipid flip-flop).<sup>[25]</sup> In the case of a transmembrane channel, the transport efficiency is not influenced by the rigidity of the membrane, whereas the chloride efflux in the case of a mobile carrier is significantly reduced. The chloride efflux obtained in EYPC and EYPC/cholesterol liposomes are summarized in Table

4 (details and graphics for these experiments available in Figures S36 - S38). No drastic decrease of the chloride efflux was observed in the presence of cholesterol, suggesting the formation of porous transmembrane architectures for both ligands.

A slight decrease of the chloride efflux efficiency in the EYPC/cholesterol liposomes for the metal assemblies was observed and may be associated to the dynamics of the self-assembly of the MOST. Indeed, the ligands may have reduced mobility inside this rigidified membrane, which may slow down the self-association process and thus, the chloride transport.

**Table 4.** Chloride efflux at 500 s obtained for ligands **1**, **2** and **3**, with or without addition of PdCl<sub>2</sub> at 270 s, in EYPC or EYPC/cholesterol liposomes

Ligand	No. of equiv. of PdCl <sub>2</sub>	EYPC	EYPC / cholesterol
		% Cl <sup>-</sup> efflux (at 500s)	% Cl <sup>-</sup> efflux(at 500s)
<b>1</b>	-	41 ± 3	40 ± 2
	0.5	50 ± 3	40 ± 3
<b>2</b>	-	30 ± 3	30 ± 3
	0.5	74 ± 4	60 ± 3
<b>3</b>	-	41 ± 2	42 ± 3
	0.5	67 ± 3	64 ± 2

The anion selectivity of the MOST was also investigated. Chloride transport was conducted in presence of different external buffer solutions. The external nitrate ion was replaced by fluoride and sulfate. The size and the hydrophilicity of the external anions had no influence on the chloride efflux in the presence of Pd<sup>2+</sup>(**3**) MOST, suggesting that a symport Cl<sup>-</sup>/cation<sup>+</sup> mechanism was dominant. However, the symport Cl<sup>-</sup>/cation<sup>+</sup> and the antiport Cl<sup>-</sup>/anion<sup>-</sup> probably occurs at the same time for Pd<sup>2+</sup>(**2**) which saw its efficiency slightly reduced in presence of fluoride and sulfate (Figure 9).

The formation of MOST in the phospholipid membrane to ensure anion transport is an important finding and our hypothesis was that a MOST could also disrupt ion homeostasis in living organisms. As we previously reported that benzimidazolium transmembrane transporters possess antimicrobials properties,<sup>[26]</sup> the toxicity of the MOST to Gram-positive wild-type and tetracycline-resistant bacteria was investigated. Our hypothesis was that if MOST can be formed in the bacterial membranes and they possess a porous structure, they could act as the hydraphiles reported by Gokel *et al.*<sup>[27]</sup>, making the bacterial membrane more permeable to ions and antibiotics.

## FULL PAPER

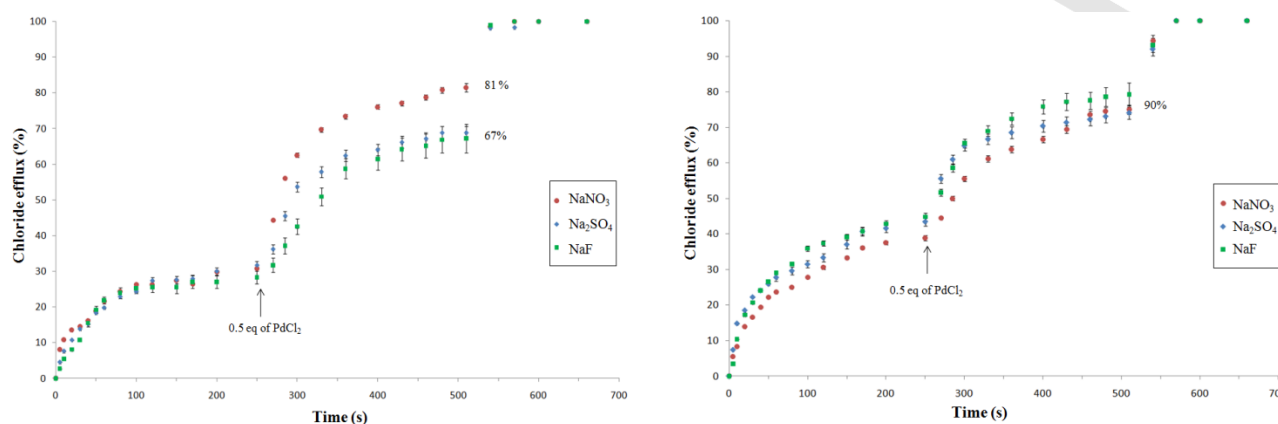


**Figure 9.** Chloride efflux obtained after the addition of 0.5 equivalents of PdCl<sub>2</sub> (relative to the concentration of the transporter) at 270 s in the presence of 12.5 mol% (relative to the EYPC concentration) of a) **2** or b) **3** in liposomes bathing in different buffers at 25°C. Triton X was added at 525 s to lyse the liposomes.

### Antimicrobial activity

The bacterial membrane is a complex environment containing different proteins and a peptidoglycan layer in addition to the phospholipid bilayer.<sup>[28]</sup> The ability of a synthetic compound to penetrate the artificial phospholipid membrane of a liposome and the one of living bacteria can be very different.

The formation of MOSTs in complex bacterial membranes, their ability to disrupt ion homeostasis and the effect on the survival rate of living bacteria were investigated. We first determined the minimum inhibitory concentration (MIC) for ligands **1**, **2** and **3** alone in Gram-positive wild-type *Bacillus thuringiensis* (HD73) (Table 5).

The first observation that can be made from this study is that the efficiency of the three ligands to transport chloride in liposomes (EC<sub>50</sub>) cannot be correlated to their ability to kill Gram-positive *B. thuringiensis* bacteria. Ligand **3** is the only one possessing a MIC of 35 - 40 μM against *B. thuringiensis*. These experiments were also performed with the preformed complex Pd<sup>2+</sup>(**2**) and Pd<sup>2+</sup>(**3**), but no difference was noted in terms of the MIC values. These results were not surprising, since we previously observed that the metal-ligand complexes were not stable in an aqueous environment. However, if 0.5 equivalent of PdCl<sub>2</sub> was added after 1 h of incubation of the bacteria with the ligand **3**, the MIC of Pd(**3**) complex was reduced 2-fold. This result demonstrates the formation of the MOST in the bacterial membrane and its capacity to alter its permeability.

Intrigued by the lack of antibacterial activity of **2** and its Pd<sup>2+</sup> complex after 24 h of incubation, we performed a kinetic experiment on the bacterial growth (Figure 10).

Addition of 0.5 equivalent of PdCl<sub>2</sub> to 25 μM of **2** results in an increase of the doubling time from 82 ± 1 min to 234 ± 1 min in the first two hours.

**Table 5.** Antimicrobial activity (MIC) and transport chloride efficacy (EC<sub>50,500s</sub>) of **1**, **2** and **3**\*

Ligand	No. of equiv. of PdCl <sub>2</sub>	Bacteria	Liposomes
		<i>B. thuringiensis</i> MIC (μM)**	EC <sub>50,500s</sub> (mol %)
<b>1</b>	-	> 100	6.9
	0.5	> 100	7.0
<b>2</b>	-	> 100	20.0
	0.5	> 100	9.5
<b>3</b>	-	35 - 40	12.6
	0.5	15 - 20	10.9

\*PdCl<sub>2</sub> was not toxic even at 100 μM (Figure S46)

\*\*100 μM was the limit of solubility in the bacterial growth media

However, in the following two hours the doubling time decreases to 77 ± 1 min, showing the disassembly of the metal-ligand complex. A more pronounced effect can be observed after the addition of the second aliquot of PdCl<sub>2</sub>, when a doubling time of 269 ± 1 min was observed. However, after 24 h of incubation, the global bacterial growth was not affected by the presence of **2** and Pd<sup>2+</sup> in solution. These kinetic experiments suggest that the Pd<sup>2+</sup>(**2**) MOST forms rapidly in the bacterial membrane but is not stable enough to persist and function over a long period of time.

The higher stability of the Pd<sup>2+</sup>(**3**) compared to Pd<sup>2+</sup>(**2**) can also be inferred from these experiments, as a notable difference in the doubling time can be observed upon the addition of the first aliquot of PdCl<sub>2</sub> to **3**. In the presence of ligand **3** alone, despite its efficacy at the beginning, bacteria entirely grown after 24 hours of

## FULL PAPER

incubation, where a complete inhibition of the bacterial growth was observed with the Pd<sup>2+</sup>(**3**) complex.

Antibiotic resistance has become a major problem in the treatment of Gram-positive bacterial infections.<sup>[29]</sup> These organisms are able to escape antibiotic activity through several mechanisms including  $\beta$ -lactamase production, altered penicillin-binding proteins, aminoglycoside-modifying enzymes, modification of the target site of the antibiotic and active efflux.<sup>[29-30]</sup> Therapeutic strategies to kill these resistant Gram-positive bacteria include the use of a higher antibiotic dosage, the use of alternative, non-conventional drugs, alone or in combination and the development of new drugs.<sup>[31]</sup> Bacteria use natural efflux pumps to eject foreign substances such as antibiotics. Based on the ability of the MOST to make the membrane permeable, we thought interesting to exploit the possibility to facilitate the passage of small antibiotic molecules in the porous architectures

they form in the bacterial membrane. To mimic a resistant strain, we used a *B. thuringiensis* tetracycline-resistant strain, possessing a plasmid that expresses an efflux pump in the bacterial membrane that limits the access of tetracycline to the ribosome.<sup>[30]</sup> The presence of this plasmid confers a resistance to tetracycline up to 670  $\mu$ M (See ESI, Figure S47).

Firstly, we determined that **3** and MOST Pd<sup>2+</sup>(**3**) at 25  $\mu$ M were non-toxic to this strain (Figure 11). As a reminder, at the same concentration, both **3** and MOST Pd<sup>2+</sup>(**3**) were toxic to the wild-type *B. thuringiensis*, but the presence of the efflux pump affects their capacity to remain into the bacterial membrane after 24 h.

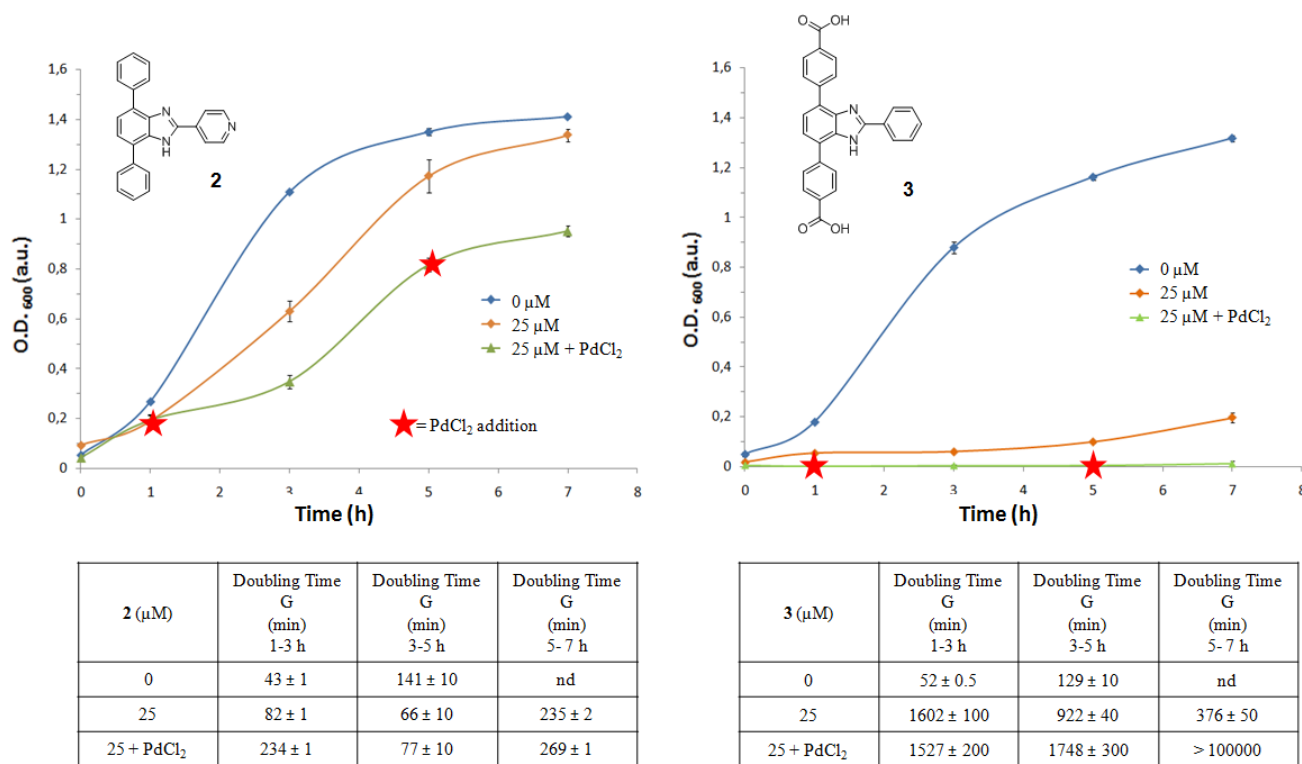


**Figure 10.** Optical density of *B. thuringiensis* obtained after several hours of incubation with different concentration of **2** and **3**. On the right, 0.5 equivalent of PdCl<sub>2</sub> (relative to the ligand concentration) was added after 1h and 5h of incubation of the ligand with bacteria. Doubling time G was defined as the time taken by bacteria to double in number during the exponential phase.  $G = t / (3.3 \log b/B)$  with  $t$  = time interval in minutes,  $b$  = number of bacteria at the end of the time interval and  $B$  = number of bacteria at the beginning of the time interval.<sup>[32]</sup>

## FULL PAPER

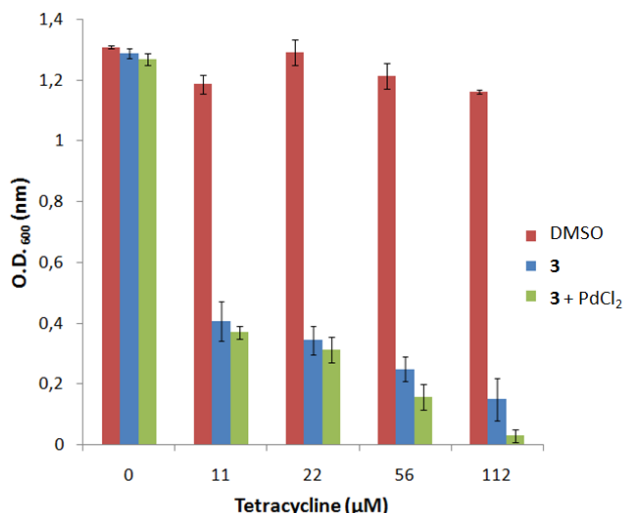


**Figure 11.** Tetracycline-resistant *B. thuringiensis* growth in presence of 5  $\mu$ l DMSO (used as a blank to monitor the effect of the DMSO on the bacterial growth) and 25  $\mu$ M of **3** (5  $\mu$ l in DMSO). The PdCl<sub>2</sub> aliquot (2.5  $\mu$ l in DMSO) was added after 1 h of incubation with **3**. Maximum of bacteria growth was measured after 24 h of incubation at 37 °C.

Bacterial growth was monitored in the presence of **3** and Pd<sup>2+</sup>(**3**) MOST at 25  $\mu$ M in the presence of different tetracycline concentrations, below the MIC (670  $\mu$ M). For each tetracycline concentration, a blank with only DMSO was performed to confirm the bacterial growth under these conditions.

As shown in Figure 11, the presence of **3** and Pd<sup>2+</sup>(**3**) MOST decreased the tolerance of these resistant bacteria to tetracycline. Pd<sup>2+</sup>(**3**) MOST appears to be more effective than **3**, being more permeable and inhibiting the bacterial growth at lower concentrations of tetracycline (Figure 11). Even at 11  $\mu$ M tetracycline (60-fold lower than the MIC), the bacterial growth rate is surprisingly reduced. The combination of 25  $\mu$ M of Pd<sup>2+</sup>(**3**) MOST and tetracycline (110  $\mu$ M) completely inhibits the bacterial growth, whereas the same concentrations of tetracycline alone have no influence on the bacterial growth of this resistant strain. It may be that formation of the Pd<sup>2+</sup>(**3**) MOST in the bacterial membrane may compensate for the tetracycline efflux induced by the pump, allowing a faster influx or an increased amount of tetracycline into the bacteria. This also suggests that MOSTs possess a porous architecture, as tetracycline, which is much larger than chloride, can be transported into bacteria. This result points to a synergy between MOST and tetracycline, demonstrating the importance and potential application of MOST as a strategy to fight resistant bacteria.

## Conclusions

We have successfully synthesized two 2,4,7-triphenylbenzimidazole derivatives and demonstrated the formation of their respective metal assemblies in phospholipid membranes. Anion transport experiments performed with these ligands and their metal complexes allowed us to show their efficiency as chloride transporters in liposomes. The formation of MOST Pd<sup>2+</sup>(**2**) and Pd<sup>2+</sup>(**3**) in the phospholipid membrane results in efficient assemblies in terms of chloride transport. We also demonstrated the insertion of the ligands and formation of their metal-organic assembly in complex bacterial membranes and successfully applied MOST to make bacterial membrane more permeable to antibiotics. Finally, as a potential strategy to combat resistant bacteria, we showed that a combination of **3** and Pd<sup>2+</sup>(**3**) with tetracycline lowers the sensitivity of resistant bacteria to tetracycline by 60-fold. Work is in progress in our group to demonstrate the generality and the therapeutic interest to use MOST in pathologically relevant resistant strains.

## Experimental Section

**Materials.** L- $\alpha$ -phosphatidylcholine was purchased from Avanti Polar Lipids and was used without further purification. All chemicals were purchased from Aldrich Chemicals in their highest purity and used without further purification. CD<sub>3</sub>OD and DMSO-*d*<sub>6</sub> were purchased from CDN Isotopes.

**Instrumentation.** NMR experiments were recorded on 400 MHz Bruker Avance 400 or Bruker Avance 700 spectrometer at 298 K. Chemical shifts are reported in ppm relative to residual coupling constants are given in Hertz (Hz). High-resolution mass spectra (HRMS) were recorded on a TSQ Quantum Ultra (thermo Scientific) triple quadrupole with accurate mass option instrument. Chloride efflux was recorded with a chloride selective micro electrode.

**Preparation of EYPC large unilamellar vesicles (LUVs):** A phospholipid film was formed by evaporating 1 ml chloroform solution containing 25 mg of EYPC, under vacuum at 25 °C during 2 hours. The lipid film was then hydrated with 1 mL of a NaCl (500 mM) and phosphate buffer solution (5 mM, pH = 7.2). The obtained suspension was subjected to at least 8 freeze/thaw/vortex cycles (1 cycle = 1 minute at -78 °C followed by 1 minute at 35 °C and 1 minute in vortex). The solution was then extruded through a 100 nm polycarbonate membrane 21 times until the solution was transparent and passed down a Sephadex G-25 column to remove extravesicular NaCl. The liposomes were eluted with a solution containing 5 mM of phosphate buffer with 500 mM of NaNO<sub>3</sub> (pH = 7.2). 4.3 mL of liposomes solution were isolated after separation. The stock solution was diluted to obtain a 5 mM lipid solution, assuming all EYPC was incorporated into the liposomes.

## FULL PAPER

**Chloride transport assays with EYPC LUVs:** A 60  $\mu\text{L}$  aliquot of the solution of EYPC LUVs (5 mM) was added to a 1.2 mL gently stirred buffer solution containing 5 mM phosphate salt and 500 mM  $\text{NaNO}_3$  (pH = 7.2). The chloride efflux was monitored as function of time by a chloride-selective electrode. 7.5  $\mu\text{L}$  of a solution of transporter at different concentrations in MeOH were added to start the transport. At  $t = 600$  s, 100  $\mu\text{L}$  of a Triton-X 5% solution were added to lyse all liposomes to obtain the maximum of chloride efflux. Experiments were repeated in triplicate and all the reported traces are the average of the three independent trials

**Minimal inhibitory concentration (MIC):** 5 mL of Lysogeny Broth (LB) medium were inoculated with *Bacillus thuringiensis* (HD73 strain). The preculture was grown overnight at 37°C under agitation at 230 RPM, and resuspended in 75 mL of a fresh LB medium. The culture was grown at 37°C during 2 more hours. After this time, the culture was diluted in fresh LB medium to obtain an OD600 of 0.1-0.2. Each well was filled with 195  $\mu\text{L}$  bacterial cultures and 5  $\mu\text{L}$  of DMSO or compounds in DMSO solution, as the final volume in each well was 200  $\mu\text{L}$  and the maximum concentration of DMSO was 5%. The plates were agitated at 230 RPM in a thermostated incubator at 37°C and the solution OD600 was monitored over time. Every experiment was repeated in triplicate on independent bacterial cultures. The MICs were determined as the minimal concentration at which no bacterial growth was detected.

## Acknowledgements

We gratefully acknowledge the Natural Sciences and Engineering Research Council of Canada (NSERC), the Fonds Québécois de la Recherche sur la Nature et les Technologies (FRQ-NT) and the Université de Montréal for the financial support. We also thank Le Centre Régional de RMN and Le Centre Régional de Spectrométrie de masse of the Université de Montréal. We thank prof. J.N. Pelletier for access to instruments in her laboratory and helpful discussion of this manuscript.

**Keywords:** metal-organic assemblies • 2,4,7-triphenyl benzimidazole • transmembrane transport • antibacterials • tetracycline

- [1] G. Ferey, *Chem Soc Rev* **2008**, *37*, 191-214.
- [2] J. R. Long and O. M. Yaghi, *Chem Soc Rev* **2009**, *38*, 1213-1214.
- [3] a) L. J. Murray, M. Dinca and J. R. Long, *Chem Soc Rev* **2009**, *38*, 1294-1314; b) R. E. Morris and P. S. Wheatley, *Angew Chem Int Ed Engl* **2008**, *47*, 4966-4981.
- [4] P. Horcajada, R. Gref, T. Baati, P. K. Allan, G. Maurin, P. Couvreur, G. Ferey, R. E. Morris and C. Serre, *Chem Rev* **2012**, *112*, 1232-1268.
- [5] P. Horcajada, C. Serre, M. Vallet-Regi, M. Sebban, F. Taulelle and G. Ferey, *Angew Chem Int Ed Engl* **2006**, *45*, 5974-5978.
- [6] N. Ahmad, H. A. Younus, A. H. Chughtai and F. Verpoort, *Chem Soc Rev* **2015**, *44*, 9-25.
- [7] E. Gouaux and R. Mackinnon, *Science* **2005**, *310*, 1461-1465.
- [8] a) P. A. Gale, N. Busschaert, C. J. E. Haynes, L. E. Karagiannidis and I. L. Kirby, *Chem.Soc.Rev.* **2014**, *43*, 205-241; b) N. Busschaert, C. Caltagirone, W. Van Rossom and P. A. Gale, *Chem. Rev.* **2015**, *115*, 8038-8155.
- [9] a) N. Sakai and S. Matile, *Langmuir*, **2013**, *29*; b) S. Matile, A. Vargas Jentzsch, J. Montenegro and A. Fin, *Chem Soc Rev* **2011**, *40*, 2453-2474; c) T. Saha, S. Dasari, D. Tewari, A. Prathap, K. M. Sureshan, A. K. Bera, A. Mukherjee and P. Talukdar, *J Am Chem Soc* **2014**, *136*, 14128-14135.
- [10] a) M. G. Fisher, P. A. Gale, M. E. Light and S. J. Loeb, *Chem Commun (Camb)* **2008**, 5695-5697; b) C. R. Bondy, P. A. Gale and S. J. Loeb, *J Am Chem Soc* **2004**, *126*, 5030-5031; c) S. Ma, M. M. Smulders, Y. R. Hristova, J. K. Clegg, T. K. Ronson, S. Zarra and J. R. Nitschke, *J Am Chem Soc* **2013**, *135*, 5678-5684.
- [11] a) O. V. Kulikov, R. Li and G. W. Gokel, *Angew Chem Int Ed Engl* **2009**, *48*, 375-377; b) M. Jung, H. Kim, K. Baek and K. Kim, *Angew Chem Int Ed Engl* **2008**, *47*, 5755-5757.
- [12] E. Mahon, S. Garai, A. Muller and M. Barboiu, *Adv. Mater.* **2015**, *27*, 5165-5170.
- [13] a) M. Boccalon, E. Iengo and P. Tecilla, *J Am Chem Soc* **2012**, *134*, 20310-20313; b) F. De Riccardis, I. Izzo, D. Montesarchio and P. Tecilla, *Acc Chem Res* **2013**, *46*, 2781-2790.
- [14] U. Devi, J. R. Brown, A. Almond and S. J. Webb, *Langmuir* **2011**, *27*, 1448-1456.
- [15] A. Satake, M. Yamamura, M. Oda and Y. Kobuke, *J Am Chem Soc* **2008**, *130*, 6314-6315.
- [16] T. M. Fyles and C. C. Tong, *New J. Chem.* **2007**, *31*, 655-661.
- [17] a) C. P. Wilson and S. J. Webb, *Chem Commun (Camb)* **2008**, 4007-4009; b) C. P. Wilson, C. Boglio, L. Ma, S. L. Cockroft and S. J. Webb, *Chemistry* **2011**, *17*, 3465-3473.
- [18] C. Janiak, *Dalton Trans.* **2003**, 2781-2804.
- [19] a) G. A. Santillan and C. J. Carrano, *Inorg Chem* **2008**, *47*, 930-939; b) M. Eddaoudi, D. B. Moler, H. Li, B. Chen, T. M. Reineke, M. O'Keefe and O. M. Yaghi, *Accounts of Chemical Research* **2001**, *34*, 319-330.
- [20] J. Kempf, N. Noujeim and A. R. Schmitzer, *RSC Adv.* **2014**, *4*, 42293-42298.
- [21] S. Medici, M. Peana, V. M. Nurchi, J. I. Lachowicz, G. Crisponi and M. A. Zoroddu, *Coordination Chemistry Reviews* **2015**, *284*, 329-350.
- [22] a) N. Noujeim, K. Zhu, V. N. Vukotic and S. J. Loeb, *Org. Lett.* **2012**, 2484-2487; b) K. Zhu, C. A. O'Keefe, V. N. Vukotic, R. W. Schurko and S. J. Loeb, *Nat Chem* **2015**, *7*, 514-519.
- [23] N. Şireci, Ü. Yılmaz, H. Küçükbay, M. Akkurt, Z. Baktir, S. Türktekin and O. Büyükgüngör, *Journal of Coordination Chemistry* **2011**, *64*, 1894-1902.
- [24] a) A. Krogul, J. Cedrowski, K. Wiktorska, W. P. Ozimińska, J. Skupińska and G. Litwinienko, *Dalton Trans.* **2012**, *41*, 658-666; b) D. Ray, J. T.

## FULL PAPER

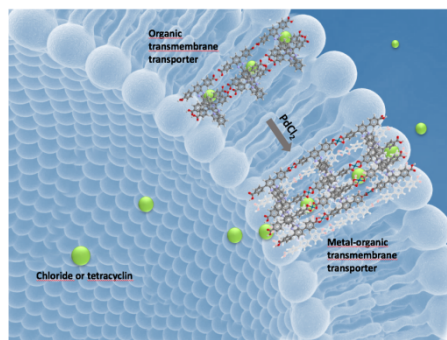
- Foy, R. P. Hughes and I. Aprahamian, *Nature Chemistry* **2012**, *4*, 757-762.
- [25] M. R. Krause and S. L. Regen, *Acc. Chem. Res.* **2014**, *47*, 3512-3521.
- [26] C. R. Elie, G. David and A. R. Schmitzer, *J. Med. Chem.* **2015**, *58*, 2358-2366.
- [27] J. L. Atkins, M. B. Patel, Z. Cusumano and G. W. Gokel, *Chem Commun (Camb)* **2010**, *46*, 8166-8167.
- [28] N. Malanovic and K. Lohner, *Biochim Biophys Acta* **2015**.
- [29] E. Bouza and R. Finch, *Clinical Microbiology and Infection* **2012**, *7*, 3.
- [30] B. S. Speer, N. B. Shoemaker and A. A. Salyers, *Clin Microbiol Rev* **1992**, *5*, 387-399.
- [31] J. M. Rybak, K. E. Barber and M. J. Rybak, *Expert Opin Pharmacother* **2013**, *14*, 1919-1932.
- [32] T. J. Daskivich, M. M. Regan and W. K. Oh, *J Urol* **2006**, *176*, 1927-1937.

## FULL PAPER

## Entry for the Table of Contents

## FULL PAPER

Formation of metal-organic synthetic transporters (MOST) in phospholipid membranes. MOST make the membranes of resistant bacteria more permeable to antibiotics. As a potential strategy to combat resistant bacteria, we demonstrate that the combination of MOST with tetracycline lowers the sensitivity of resistant bacteria by 60-fold.



Julie Kempf, Andreea R. Schmitzer\*

Page No. – Page No.

**Metal-organic synthetic transporters (MOST): efficient chloride and antibiotic transmembrane transporters**